Computer Fraud and Security
ISSN (online): 1873-7056

Design and Verification of Intelligent Driving Braking Energy System Based on Model Predictive Control

Jun Wang, Tianhui Li, Yongbin Liang*, Tao Chen, Hong Zhang, Yanli Li
SAIC-GM-Wuling Automobile Company Limited, Liuzhou 540057, Guangxi, China
**Corresponding Author.*

Abstract:
Given that the actual endurance Mileage of the vehicle is much lower than the theoretical endurance Mileage under the traditional intelligent driving mode, this paper develops an Adaptive Cruise Control (ACC) model based on dynamic predictive time-domain management. The developed Adaptive Cruise Control model is not only considering actuator efficiency and time delay, but also improving system safety by predicting the vehicle's motion state. This paper also verifies the feasibility of the Adaptive Cruise Control Model through simulation conditions by building a hardware in the loop simulation test platform based on Carsim/Veristand/MATLAB. It will use test platform conducting virtual simulations of cruise control acceleration, deceleration, and stopping to verify the effectiveness and accuracy of the intelligent driving system based on model predictive control. It also compares and verify the system designed in this paper on a real vehicle with the operating conditions of adaptive cruise control, start && stop, and China Light-duty Vehicle Test Cycle (CLTC). It turns out that the overall comprehensive endurance Mileage of intelligent driving was improved by 17.5% after adding energy recovery mode. And energy consumption reduces by 1.75 kwh per 100 kilo meters. The braking deceleration process is more linear, with a comfort level improvement of 6.46%, an average deceleration reduction by 0.2m/s^2, and an average reduction of 4bar in maximum braking pressure, further avoiding braking energy loss.

Keywords: intelligent driving, model predictive control, dynamic time-domain management, adaptive cruise control, energy recover

INTRODUCTION

From January to October 2023, the penetration rate of intelligent driving L2 models increased significantly from 39.9% in January to 50.6% in October. At present, L2 configuration is gradually replacing "camera plus radar solution" with "single camera solution", and low-cost while high-value intelligent driving configuration has become the goal pursued by various car companies. The national manufacturing and automotive innovation development strategies both clearly state the need to strengthen the independent research and development of key core technologies and key components of electric intelligent connected vehicles, achieve technological self-reliance and self-improvement, strengthen and expand national brands, and become an important measure to promote the high-quality development of China's automotive manufacturing industry, build a strong country in science and technology, and strengthen the automotive industry [1]

The actual endurance Mileage of a certain car model when Adaptive Cruise Control is turned on is much lower than the theoretical endurance Mileage, with an achievement rate of less than 87%. Compared to manual driving conditions, the achievement rate of endurance Mileage is reduced by 5.7%. According to the principle of energy recovery and the analysis of vehicle energy flow, when energy recovery is turned on, the actual endurance Mileage of the vehicle increases by more than 20% compared to when energy recovery is turned off. This indicates that the endurance Mileage can be improved by optimizing the vehicle control strategy and energy recovery mode in Adaptive Cruise Control mode.

Li et al. developed an adaptive cruise control system based on iterative learning method, and simulations showed that the expected acceleration tracking effect was better in dynamic tracking. Its disadvantage is that the Adaptive Cruise Control algorithm is only for short-term predictions and the Model Predictive Control model requires high computing power [2-5]. Ren et al. designed a longitudinal control algorithm based on the feedforward and (Back Propagation,BP)-(Proportional-Integral-Derivative,PID) feedback control law of vehicle longitudinal dynamics, and compared it with the feedforward and PID feedback algorithm through simulation. This control algorithm can achieve more accurate tracking of expected acceleration. Compared with the linear quadratic regulato algorithm, the following performance has been improved by 22.6%, and the economy has been improved by 2.9%, meeting

the multi-objective requirements of longitudinal following of vehicles [6]. The Adaptive Cruise Control system designed by Li et al. based on fuzzy logic and sliding mode control theory can maintain good tracking and adaptability of vehicles under acceleration and deceleration conditions [7]. Based on the principle of longitudinal dynamics of vehicles, Fancher et al. established an inverse dynamics model for driving and braking, which enables the system to follow the expected acceleration stably and quickly. The instability of the model is compensated for through algorithms, and simulation results show that acceleration tracking control is more accurate [8,9]. Moser D et al. take the power consumption of electric vehicles as the economic target, model predictive control is used to optimize the following economy. The results show that compared with the linear quadratic regulato control algorithm, using the model predictive control algorithm can significantly improve the following economy [10-12].Hu Ji adopts dynamic programming to design the Adaptive Cruise Control control strategy for hybrid vehicles, and simulation results show that the algorithm has better economic benefits [13,14].Sun et al. Wei Xin, and others achieved longitudinal acceleration following control of vehicles through torque control using a vehicle dynamics model with feedforward and PID feedback. However, the system did not consider the impact of actuators on control accuracy and lacked strong real vehicle validation [15-19].

From the research situation, most Adaptive Cruise Control systems are designed through feedback control PID algorithm, focusing on the tracking and economy of the acceleration system, and verified through simple cruise conditions such as following stop through simulation, lacking strong verification of endurance Mileage and energy consumption optimization. This article comprehensively considers the issues of actuator delay and efficiency, and designs an intelligent driving braking energy control system based on model predictive control. The reliability of the system is verified through a hardware in the loop system, and a China Light-duty Vehicle Test Cycle test is conducted on a certain vehicle model. The test results show that under intelligent driving mode, the comprehensive endurance Mileage improvement and braking comfort of intelligent driving can be achieved by calibrating parameters and changing algorithm modes.

INTELLIGENT DRIVING BRAKING AND POWER ENERGY RECOVERY MODEL

System Solution

The design of the intelligent driving drive and braking energy system is divided into two parts. The working system diagram is shown in Figure 1, which is usually divided into a decision control layer and an execution layer. Each part is designed based on modular theory, and its work is relatively independent, improving the flexibility and universality of each module [20-22]. The perception layer inputs monitoring of driving environment information and the vehicle's own state. The decision layer and control layer process the target information input from the perception layer and output the expected acceleration for control. After receiving the expected acceleration control signal from the ACC decision control layer, the execution layer intervenes in the vehicle's drive system actuators and brake actuators based on the information input from the perception end, so that the actual acceleration of the vehicle follows the expected acceleration output of the ACC decision as much as possible. The system is fast, stable, and accurate, such as the pressure braking of EBS and the braking or VCU driving brought by VCU energy recovery.

Predictive Longitudinal Control Algorithm

The strategy of ACC system control is to control the actuators of the vehicle so that the acceleration of the vehicle quickly and stably follows its output desired acceleration. The decision control layer collects information on the speed, driving torque, acceleration, and braking pressure of the ego vehicle, and processes it through the perception layer to collect information on the distance and speed of the target vehicle. It predicts the motion status of the ego vehicle and the target vehicle, considers the issues of actuator delay and efficiency, and uses the sliding control principle to constrain acceleration changes for system execution planning and decision-making, and outputs the expected acceleration. The execution layer converts the driving torque required for vehicle acceleration and the negative torque and braking pressure required for braking through the inverse longitudinal dynamics model, achieving the goal of following the expected acceleration of the vehicle and ensuring the accuracy and safety of the ACC system.

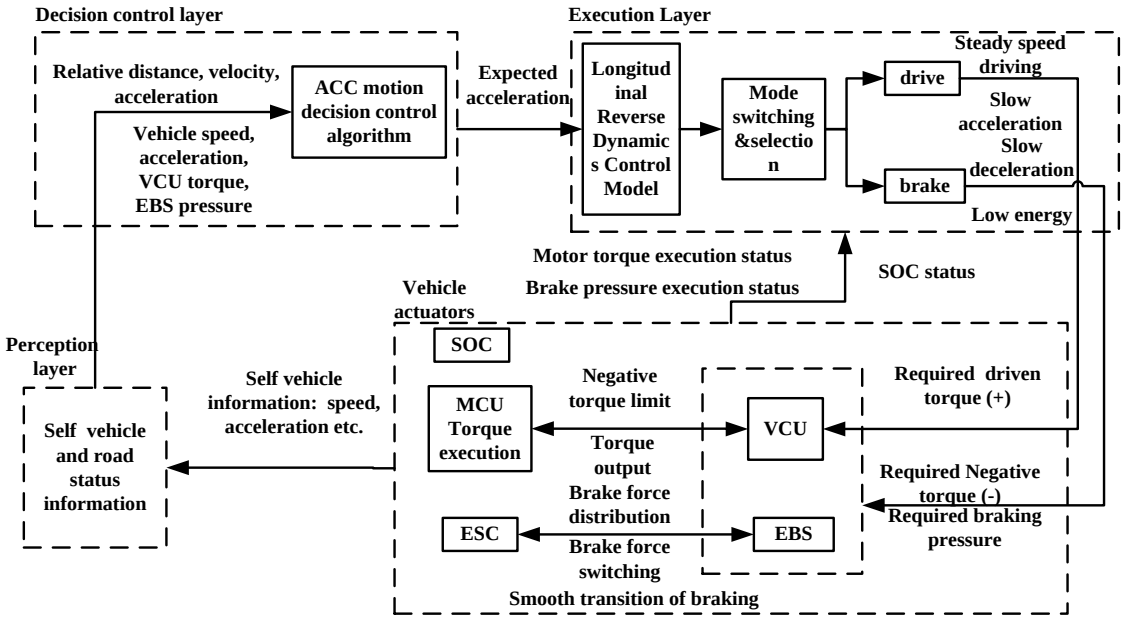

Figure 1 ACC working system diagram

Acceleration planning of car following

Estimate the acceleration of the vehicle based on the current velocity of the target object and the velocity from the previous moment. Considering the control error caused by actuator delay, predict the speed, acceleration, and distance of the target and the vehicle. Then, using the idea of MPC, dynamically optimize the time interval of the self-driving vehicle. At the same time, the acceleration change rate of the vehicle is calculated to achieve constrained optimization of acceleration and output the final expected acceleration.

Processing of relative distance with the vehicle:Due to that some intelligent driving sensors perceive and measure relative distancesL_{IV} may jump when the vehicle comes to a stop,when the forward vehicle is detected to be stationary or Speed less than the calibration valueV_h,Maintain the distanceL_{IV} from the previous moment,denoted asL_{IVPos},V_h is the real-time speed of the vehicle.

Target vehicle acceleration processing

Target vehicle acceleration $a_{\mathrm{TgtVehFlt}}$ processing:Mainly includes target vehicle acceleration correction, acceleration compensation, and acceleration filtering.

Target vehicle acceleration correction:The acceleration is integrated to obtain the estimated speed of the target vehicle $V_{\mathrm{TgtVehEst}}(k)$,among them, the initialization condition for integration is either no target vehicle or switching target vehicle IDs,the initialization value is the perceived speed of the target vehicle V_{TgtVeh}.Difference between $V_{\mathrm{TgtVehEst}}(k)$ andV_{TgtVeh} to obtain speed error,estimation error of target vehicle acceleration through proportional operation$a_{\mathrm{TgtVehErr}}(k)$. Use this error to correct the acceleration perception input value of the target vehicle $a_{\mathrm{TgtVehInput}}(k)$, Obtain unfiltered target vehicle acceleration correction value $a_{\mathrm{TgtVehUnflt}}(k)$,Participate in the next integral cycle calculation. At the same time, the final target vehicle acceleration correction value is obtained through first-order filtering operation $a_{\mathrm{TgtVehMfd}}(k)$. The above correction process can be represented by the following equation:

$$V_{\mathrm{TgtVehEst}}(0) = V_{\mathrm{TgtVeh}}(0) \tag{1}$$

$$V_{\mathrm{TgtVehEst}}(k) = a_{\mathrm{TgtVehUnflt}}(k-1) \cdot T + V_{\mathrm{TgtVehEst}}(k-1) \tag{2}$$

$$a_{\mathrm{TgtVehErr}}(k) = (V_{\mathrm{TgtVehEst}}(k) - V_{\mathrm{TgtVeh}}(k)) \cdot p_{gain} \tag{3}$$

$$a_{\mathrm{TgtVehUnflt}}(k) = a_{\mathrm{TgtVehInput}}(k) - a_{\mathrm{TgtVehErr}}(k) \tag{4}$$

$$a_{\text{TgtVehMfd}}(k) = k_{flt} a_{\text{TgtVehUnflt}}(k) + (1 - k_{flt}) a_{\text{TgtVehUnflt}}(k-1) \tag{5}$$

In the above equation, represents the sampling period,p_{gain} indicate gain coefficient,k_{flt} indicate the filtering coefficient,The discrete integral operation adopts the forward Euler method.

Perform variable weight summation on $a_{\text{TgtVehMfd}}$ and $a_{\text{TgtVehInput}}$, Set different weights based on different vehicle models and scenarios,Multiply the corresponding weights by $a_{\text{TgtVehMfd}}$, $a_{\text{TgtVehInput}}$ and then add them up. The calculation process can be represented by the following equation:

$$a_{\text{TgtVehWtd}}(k) = w_1 a_{\text{TgtVehInput}}(k) + w_2 a_{\text{TgtVehMfd}}(k) \tag{6}$$

Target acceleration compensation and filtering: In order to cope with extreme scenarios such as rapid deceleration of the target vehicle, it is necessary to perform appropriate gain compensation on the acceleration of the target vehicle to improve the driving safety of the following vehicle. The weighted acceleration value of the target vehicle and the ego vehicle speed are used as two-dimensional information inputs for gain compensation processing, and the gain value is adjusted based on the differences in vehicle model parameters and target vehicle acceleration accuracy. To eliminate acceleration fluctuations caused by acceleration gain compensation, it is necessary to perform amplitude limiting and filtering processing to smooth the calculated acceleration value of the target vehicle and obtain the target acceleration value required by the subsequent following acceleration planning processing module $a_{\text{t\_prcd}}(k)$.The calculation process of target acceleration compensation and filtering can be represented by the following equation:

$$\tilde{a}_{\text{t\_prcd}}(k) = min\{max\{[a_{\text{TgtVehWtd}}(k) \cdot p(a_{\text{TgtVehWtd}}(k), V_h(k))], a_{\text{lo}}\}, a_{\text{up}}\} \tag{7}$$

$$a_{\text{t\_prcd}}(k) = \tilde{k}_{\text{flt}} \tilde{a}_{\text{t\_prcd}}(k) + (1 - \tilde{k}_{\text{flt}}) \tilde{a}_{\text{t\_prcd}}(k) \tag{8}$$

$$a_{\text{TgtVehFlt}}(k) = a_{\text{t\_prcd}}(k) \tag{9}$$

Processing of actuators delay

The actuators of the vehicle have response delays and errors. Adding an efficiency and delay prediction processing step to the actuators can predict the relative motion state between the ego vehicle and the target vehicle after delayed response, which can more accurately plan the acceleration of the following vehicle. The steady-state error of the actuator response characterizes the execution efficiency of the expected acceleration of the vehicle, while the execution efficiency of the driving brake is often different,Represented by e_{brk} and $e_{acceltn}$,estimate the expected acceleration of the vehicle's actual execution, which can be expressed by the following equation:

$$a_{\text{hfe}}(k) = \begin{cases} a_{\text{hf}}(k) \cdot e_{\text{brk}}, & a_{\text{hf}}(k) < 0; \\ a_{\text{hf}}(k) \cdot e_{\text{acceltn}}, & a_{\text{hf}}(k) \geq 0; \end{cases} \tag{10}$$

By estimating the delay period of the self-driving brake actuator, predict the speed and relative distance between the self-driving vehicle and the target vehicle. The prediction process can be represented by the following equation:

$$V_{\text{h\_prdt}}(k) = max\{[V_h(k) + \sum_{i=1}^{N} a_{\text{hfe}}(k-i) \cdot T], 0\} \tag{11}$$

$$V_{\text{TgtVehPrdt}}(k) = max\{[V_{\text{TgtVeh}}(k) + \sum_{i=1}^{N} a_{\text{t\_prcd}}(k) \cdot T], 0\} \tag{12}$$

$$\begin{aligned} L_{\text{IVPosPrdt}}(k) = L_{\text{IVPos}}(k) + \sum_{j=1}^{N} \Bigg(& \max\left\{ \left[V_{\text{TgtVeh}}(k) + \sum_{i=1}^{j} a_{\text{t\_prcd}}(k) \cdot T \right], 0 \right\} - \\ & \max\left\{ \left[V_{\text{h}}(k) + \sum_{i=1}^{j} a_{\text{hfe}}(k-i) \cdot T \right], 0 \right\} \Bigg) \cdot T \end{aligned} \tag{13}$$

Where N represents the delay period of the actuator, $V_{\text{h\_prdt}}(k)$ is the predicted speed of the ego vehicle,$V_{\text{TgtVehPrdt}}(k)$ is the predicted speed of the target vehicle,$L_{\text{IVPosPrdt}}(k)$ is the relative predicted distance between the ego vehicle and the target vehicle.

Expected acceleration calculation for following the car

Dynamic Time Domain Management: Dynamic time domain management consists of normalized relative velocity and distance, as well as adaptive dynamic time domain gain factor processing. Normalization of relative velocity and relative distance divides the relative motion state between the ego vehicle and the target vehicle into two dimensions: velocity and distance. This allows for a more reasonable design of dynamic time-domain gain factors, resulting in highly adaptable prediction time domains. The normalization process is represented by the following equation:

$$R_{vr}(k) = \frac{V_{\text{TgtVehPrdt}}(k) - V_{\text{h\_prdt}}(k)}{\sqrt{V_{\text{h\_prdt}}(k)}} \tag{14}$$

$$R_{sr}(k) = \frac{L_{\text{IVPosPrdt}}(k)}{L_{\text{IVDmd}}(k)} - 1 \tag{15}$$

In the equation,L_{IVDmd} represents the expected distance between the ego vehicle and the target vehicle at different set distances, $R_{vr}(k)$ is the normalized representation of relative velocity,$R_{sr}(k)$ is a normalized representation of relative distance.

Dynamic time-domain gain factor $t_{\text{g1}}(k)$ calculation: Determining the dynamic time-domain gain factor by normalizing the two dimensions of relative velocity and relative distance $t_{\text{g1}}(k).R_{vr}(k)$ and $R_{sr}(k)$ represent the x-axis and y-axis, respectively, can be divided into four quadrants. The first quadrant represents that the relative velocity between the ego vehicle and the target vehicle is greater than zero and the relative distance is greater than the expected distance at the set time distance. The second quadrant represents that the relative speed between the ego vehicle and the target vehicle is less than zero and the relative distance is greater than the expected distance at the set time. The third quadrant represents that the relative speed between the ego vehicle and the target vehicle is less than zero and the relative distance is less than the expected distance at the set time. The fourth quadrant represents that the relative speed between the ego vehicle and the target vehicle is greater than zero and the relative distance is less than the expected distance at the set time.

Dynamic time-domain gain factors can be designed differentially according to the project requirements of different vehicle models in different quadrants $t_{g1}(k)$, The expression is as follows:

$$t_{\text{g1}}(k) = t_{g1}(R_{vr}(k), R_{sr}(k)) \tag{16}$$

To reduce the calibration workload of adapting the dynamic time-domain gain factor $t_{\text{g1}}(k)$ to different vehicle models, a dynamic time-domain gain factor $t_{\text{g2}}(k)$,for predicting the speed function of the self-driving vehicle was designed, and its expression is as follows:

$$t_{\text{g2}}(k) = t_{\text{g2}}(V_{\text{h\_prdt}}(k)) \tag{17}$$

For different vehicle models, different sizes of gain factors$t_{\text{g2}}(k)$ can be designed at different speed ranges without changing the dynamic time-domain gain factor $t_{\text{g1}}(k)$ to meet the requirements of car following in all scenarios. Combining dynamic time-domain gain factor $t_{\text{g1}}(k)$ and dynamic time-domain gain factor $t_{\text{g2}}(k)$,the total dynamic time-domain gain factor $t_g(k)$ is represented by the following equation:

$$t_g(k) = t_{\text{g1}}(k) \cdot t_{\text{g2}}(k) \tag{18}$$

The distance from a point on the xy two-dimensional coordinate system divided by $R_{vr}(k)$ and $R_{sr}(k)$ to the origin can be expressed by the following equation:

$$r_t(k) = \sqrt{(R_{vr}(k))^2 + (R_{sr}(k))^2} \tag{19}$$

The adaptive calculation for dynamic prediction in the time domain is as follows:

$$t_{\text{prdt}}(k) = t_g(k) \cdot \sqrt{r_t(k)} \tag{20}$$

Calculation of expected acceleration for following the vehicle: Based on the motion state of the vehicle, the following kinematic equations can be obtained:

$$j(t) = j_0 \tag{21}$$

$$a_h(t) = \int_{t_0}^{t_{\text{prdt}}} j_0 dt = j_0 t + a_{\text{DmdFllw}} \tag{22}$$

$$V_h(t) = \int_{t_0}^{t_{\text{prdt}}} a_h(t) dt = \frac{1}{2} j_0 t^2 + a_{\text{DmdFllw}} t + V_0 \tag{23}$$

$$L(t) = \int_{t_0}^{t_{\text{prdt}}} V_h(t) dt = \frac{1}{6} j_0 t^3 + \frac{1}{2} a_{\text{DmdFllw}} t^2 + V_0 t + L_0 \tag{24}$$

The kinematic equation constraints are as follows:

$$V(t=0) = V_0 \tag{25}$$

$$L(t=0) = L_0 = 0 \tag{26}$$

$$V(t = t_{\text{prdt}}) = V_{\text{TgtVeh}}(t_{\text{prdt}}) \tag{27}$$

$$L(t = t_{\text{prdt}}) - L_0 = L_{\text{IVPosPrdt}}(t_{\text{prdt}}) - L_{\text{IVDmd}}(V_{\text{TgtVeh}}(t_{\text{prdt}})) \tag{28}$$

From the above equation, we can obtain:

$$\begin{aligned} j_0 &= \frac{-2[a_{\text{DmdFllw}} \cdot t_{\text{prdt}} - (V_{\text{TgtVeh}}(t_{\text{prdt}}) - V_0)]}{t_{\text{prdt}}^2} \\ a_{\text{DmdFllw}} &= \frac{2 \cdot L_{\text{IVPosPrdt}}(t_{\text{prdt}})}{t_{\text{prdt}}^2} - \frac{1}{3} j_0 t_{\text{prdt}} - \frac{2 \cdot V_0}{t_{\text{prdt}}} \end{aligned} \tag{29}$$

Acceleration change rate calculation for following the vehicle

When the target is not switched, calculate the acceleration change rate of the following vehicle: By combining the a_{DmdFllw} calculated in this section with the acceleration $a_{\text{pre\_shapd}}$, calculated by the expected acceleration calculation module at the previous moment, determine the acceleration state of the vehicle at this time. The acceleration change rate calculation strategy is as follows:

$$\alpha_{\text{interp}} = \frac{V_h - V_{\text{Bkpt0}}}{V_{\text{Bkpt1}} - V_{\text{Bkpt0}}} \tag{30}$$

$$\alpha_{\text{inv}} = 1 - \alpha_{\text{interp}} \tag{31}$$

$$\dot{a}'_{\text{NrmFllw}} = \begin{cases} \dot{a}_{\text{Out}} & , \ \left(a_{\text{DmdFllw}} - a_{\text{pre\_shapd}}\right) > k_{\text{CutOut}} \ \&\& \text{ACCBrkCntrlActv} = 0 \\ \max((\alpha_{\text{interp}} \cdot k_{\text{apv1}} + \alpha_{\text{inv}} \cdot k_{\text{apv2}}), \dot{a}_{\text{FNrmFllw}}), & \left(a_{\text{DmdFllw}} - a_{\text{pre\_shapd}}\right) > k_{\text{DrvOut}} \\ \dot{a}_{\text{FNrmFllw}} & , \ \left(a_{\text{DmdFllw}} - a_{\text{pre\_shapd}}\right) <= k_{\text{DrvOut}} \ \| \ \text{ACCBrkCntrlActv} = 1 \end{cases} \tag{32}$$

In the above equation, $k_{\text{apv1}}, k_{\text{apv2}}$ represent coefficients. $\dot{a}_{\text{FNrmFllw}}$ represents the rate of change in the acceleration of the main vehicle when considering ACC braking . $V_{\text{Bkpt0}}, V_{\text{Bkpt1}}$ represents the speed calibration value, $V_{\text{Bkpt1}} > V_{\text{Bkpt0}}$; $\alpha_{\text{interp}}, \alpha_{\text{inv}}$ Interpolation coefficient representing speed. $k_{\text{CutOut}}, k_{\text{DrvOut}}$ Indicate the calibration value.

When switching targets, the calculation of the following acceleration change rate: Considering that there may be sudden external vehicles cutting in and out during the following process, in order to avoid sudden acceleration or deceleration of the following vehicle, the following acceleration change rate is processed to obtain $\dot{a}_{\text{NrmFllwNwTgt}}$, The specific design is as follows:

$$\dot{a}_{\text{NrmFllwNwTgt}} = \dot{a}'_{\text{NrmFllw}} \cdot \dot{a}_{\text{NrmFllwNwTgt1}}(L_{\text{IVPos}}, T_{\text{TgtNewDur}}) \cdot \dot{a}_{\text{NrmFllwNwTgt2}}(V_{\text{IVRltv}}, T_{\text{TgtNewDur}}) \tag{33}$$

In the above equation, $\dot{a}_{\text{NrmFllwNwTgt1}}(L_{\text{IVPos}}, T_{\text{TgtNewDur}})$ Refer to the table for the rate of change in following based on relative distance and the time of appearance of the target object, $\dot{a}_{\text{NrmFllwNwTgt2}}(V_{\text{IVRltv}}, T_{\text{TgtNewDur}})$ Refer to the table for the rate of change in following based on relative velocity and the time of appearance of the target object.

Acceleration constraint for following the vehicle

When the target is not switched, calculate the following acceleration constraint:

$$\begin{aligned} a_{\text{ShpdFllwDmdAccV1Up}} &= a_{\text{pre\_shapd}} + \dot{a}'_{\text{NrmFllw}} \cdot T & a_{\text{DmdFllw}} &> a_{\text{ShpdFllwDmdAccV1Up}} \\ a_{\text{ShpdFllwDmdAccV1}} &= a_{\text{DmdFllw}} & a_{\text{ShpdFllwDmdAccV1Low}} &\le a_{\text{DmdFllw}} \le a_{\text{ShpdFllwDmdAccV1Up}} \\ a_{\text{ShpdFllwDmdAccV1Low}} &= \max(a_{\text{MaxDecelOut}}, (a_{\text{pre\_shapd}} - \dot{a}'_{\text{NrmFllw}} \cdot T)) & a_{\text{DmdFllw}} &< a_{\text{ShpdFllwDmdAccV1Low}} \end{aligned} \tag{34}$$

In the above equation, $a_{\text{ShpdFllwDmdAccV1}}$ representing the calculated expected acceleration for following the vehicle, $a_{\text{ShpdFllwDmdAccV1Up}}$ Indicate the upper limit of expected acceleration for following the vehicle, $a_{\text{ShpdFllwDmdAccV1Low}}$ Indicates the lower limit value of the expected acceleration for following the vehicle.

When switching targets, calculate the following acceleration constraint:

$$a_{\text{ShpdFllwDmdNewTgt}} = max(a_{\text{ShpdFllwDmdAccV1}}, (a_{\text{pre\_shapd}} - \dot{a}_{\text{NrmFllwNwTgt}}) \cdot T) \tag{35}$$

In the above equation, $a_{\text{ShpdFllwDmdNewTgt}}$ When there is a new target, calculate the expected acceleration for following the vehicle.

Therefore, the expected acceleration for multi-target car following is:

$$a_{\text{fnl}} = \min\{a_{SgpdFllDmdAccV1}, \ a_{\text{SgpdFllwDmdNewTgt}}\} \tag{36}$$

Drive/Brake Switching Logic

The stacked braking energy recovery system scheme can achieve braking by controlling the motor, but considering that the ACC system requires the braking system to have the ability to actively brake, quickly increase pressure during emergency braking, and accurately control pressure. Considering that motor braking is limited by battery charging power and cannot achieve fast and high-intensity braking. Secondly, the response rate of motor braking torque is slow, making it impossible to achieve emergency braking. Therefore, a reasonable strategy for switching between driving and braking modes can help improve system control accuracy by improving the control strategies and methods of ACC and actuators, and considering the maximum range mode, the vehicle's range can be increased in intelligent driving mode.

Vehicle control is a dynamic process that requires consideration of wind resistance, rolling resistance, uphill and downhill conditions during driving. Therefore, it is not possible to simply judge acceleration and deceleration based on positive or negative acceleration. By testing the vehicle under various steady speed conditions, obtained the acceleration values av corresponding to each vehicle speed. To avoid frequent switching of control modes that may affect the driving experience, set a hysteresis interval 2az1(az1 is generally 0.1m/s^2~0.2m/s^2) on the av curve, Improve the smoothness of system control mode switching.

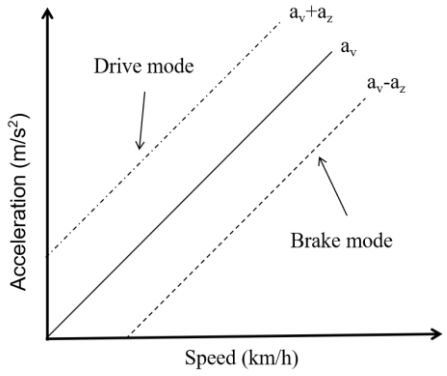

Figure 2. Drive brake switching logic diagram

Figure 2 shows the logic diagram of driving and braking switching. When the expected acceleration value is greater than av+az1, the vehicle switches to drive control for acceleration. When the expected acceleration value is less than av-az1, the vehicle switches to brake control and performs braking deceleration. When the expected acceleration is between av-az1 and av+az1, the vehicle maintains its original control mode unchanged.

$$\begin{cases} a_{fnl} > a_v + a_z; & \text{Drive mode} \\ a_v - a_z < a_{fnl} < a_v + a_z; & \text{Maintain the original mode} \\ a_{fnl} < a_v - a_z; & \text{Brake mode} \end{cases} \tag{37}$$

Braking energy recovery control strategy

Acceleration allocation: When the system switches to braking mode, precise braking force allocation strategy helps to maximize the use of motor braking force while ensuring safety, improve energy recovery efficiency, and enhance driving experience. During the actual vehicle calibration, the braking performance of the motor will be tested, and the deceleration a_{tq} size can be executed under different torques and slopes. Taking into account the maximum deceleration time at different SOC and speeds, there will be limitations on the driving force required by VCU to execute braking. To avoid frequent switching between driving and braking mode, set a hysteresis interval a_s $2a_z$(a_z is generally 0.1m/s^2~0.2m/s^2).

When SOC<13% or SOC>90%, All requests for pressure braking. When13%<SOC<90%,allocate the brake force request.

$$\begin{cases} a_{fnl} < a_{tq} - a_{z1}; & \text{Negative torque braking} \\ a_{tq} - a_{z1} < a_{fnl} < a_{tq} + a_{z1}; & \text{Hybrid braking} \\ a_{fnl} > a_{tq} + a_{z1}; & \text{Pressure braking} \end{cases} \tag{38}$$

Consider the scenario of ACC stop and go, where the drive motor frequently switches between forward and reverse directions, affecting the motor's lifespan. Therefore, when the system is below a certain speed, it will switch to pure pressure braking regardless of the state.

Drive inverse dynamics model

The core of the braking energy recovery control strategy lies in controlling the braking force of the driving motor during the vehicle braking process. According to the longitudinal driving equation of the vehicle:

$$F = F_q + F_k + F_f + F_z \tag{39}$$

F is the driving force acting on the driving wheels of the vehicle. F_q represents the rolling resistance of the vehicle. F_k is the air resistance;F_p is the slope resistance. F_z is the acceleration resistance that a car needs to overcome when accelerating.

driving force F is the torque generated by the motor transmitted to the driving wheels through the transmission system, and the specific calculation formula is as follows.

$$F = \frac{T i_c . i_j . \beta}{r}. \tag{40}$$

In the formula, T is the engine torque, i_c is the transmission ratio of the gearbox, i_j is the main reduction transmission ratio, βis the mechanical efficiency of the transmission system, r is the rolling radius of the wheels, and for rolling resistance:

$$F_q = T_l . q \tag{41}$$

In the formula, Tl is the wheel load, q is the rolling resistance coefficient, and the empirical value is between 0.01−0.018, For air resistance:

$$F_k = \frac{1}{2} . k . s . \rho . v_x^2 \tag{42}$$

In the formula, k is the air resistance coefficient. s is the area of the windward side of the car. ρ is the air density, generally ρ=1. 2258N.s^2.m-4;v_x is the relative vehicle speed,for slope resistance:

$$Ff = G.\sin\alpha \tag{43}$$

In the formula G represents the gravity acting on the car, αrepresents the slope angle.

For driving resistance:

$$F_z = \gamma.m.a_{fnl} \tag{44}$$

In the formula γ is the conversion factor for the rotational mass of the car. m is the car quality, a_{fnl} is the multi-objective expected acceleration for following the car output by the decision-making layer. Therefore, the expected torque of VCU is obtained:

$$T = \frac{\left(T_l.q + \frac{1}{2}.k.s.\rho.v_x^2 + G.\sin\alpha + \gamma.m.a_{fnl}\right)}{i_c.i_j.\beta} \tag{45}$$

Braking inverse dynamics model: The motion expression of the vehicle deceleration process can be expressed as:

$$\gamma.m.a_{fnl} = F - F_b - F_q - F_k - F_f \tag{46}$$

In the formula, Fb represents the expected braking force, and the expected braking torque is expressed as follows:

$$Fb = -m.afnl - \frac{1}{2}.k.s.\rho.v_x^2 - T_l.q \tag{47}$$

There is usually a linear relationship between the braking force Fb and the braking pressure P:

$$F_b = k.P \tag{48}$$

k is a linear coefficient, therefore:

$$P = \frac{1}{k}.\left(-m.afnl - \frac{1}{2}.k.s.\rho.V_x^2 - T_l.q\right) \tag{49}$$

HARDWARE IN THE LOOP SIMULATION

After completing the design of an adaptive cruise control system based on model predictive control, the Carsim vehicle model was used on the HIL hardware in the loop simulation platform. A corresponding vehicle control module was established in the Matlab/Simulink environment to establish a system simulation control model. The torque response, braking follow-up, cruise control and other related parameters were analyzed to verify the effectiveness and reliability of the system.

Hardware Setup

Figure 3 shows the hardware and system principles of the hardware in the environment simulation platform. The simulation platform uses a real autonomous driving controller as the test object, and is matched with virtual scene simulation, real-time simulation system, and environment perception simulation system on the periphery to jointly construct a virtual operating environment for the test controller. It mainly consists of a virtual scene simulation system, real-time simulation system, upper computer system, perception simulation system, and motor and pressure brake controller. The torque request command issued by the system is executed by VCU, and the pressure request command issued is executed by EBS.

Simulation Comparison

Combined with daily ACC usage scenarios,design simulated operating conditions such as cruise, stop-go, etc. Observe the following distance, acceleration tracking, steady-state speed, requested and responded driving torque, and requested and responded braking pressure tracking control effect of the entire vehicle.

Set the initial cruising speed to 10km/h. When the system reaches steady state, set the cruising target speed to 30km/h and 60km/h, and then gradually slowed down to 30km/h and 10km/h. The simulation results of cruise control conditions are shown in Figure 4. The system can quickly execute the expected speed, and the actual speed quickly converges to the expected vehicle speed in a short period of time, with a deviation of ± 1km/h, completing speed tracking control in acceleration scenarios. The torque variation of the motor during acceleration and deceleration closely follows the requested torque, with a tracking error of less than 100ms, a tracking error of less than 3%, and an overshoot of less than 3%. Acceleration and uniform speed control are achieved by controlling the motor, and deceleration control is achieved through negative torque. When the deceleration is low, the system uses torque to perform sliding deceleration, and the torque trend is basically consistent with the acceleration change trend of the system. At the same time, the brake pressure remains at 0 during light deceleration, which is consistent with the design and further proves that the system has a good tracking effect on the set cruise speed during acceleration and deceleration.

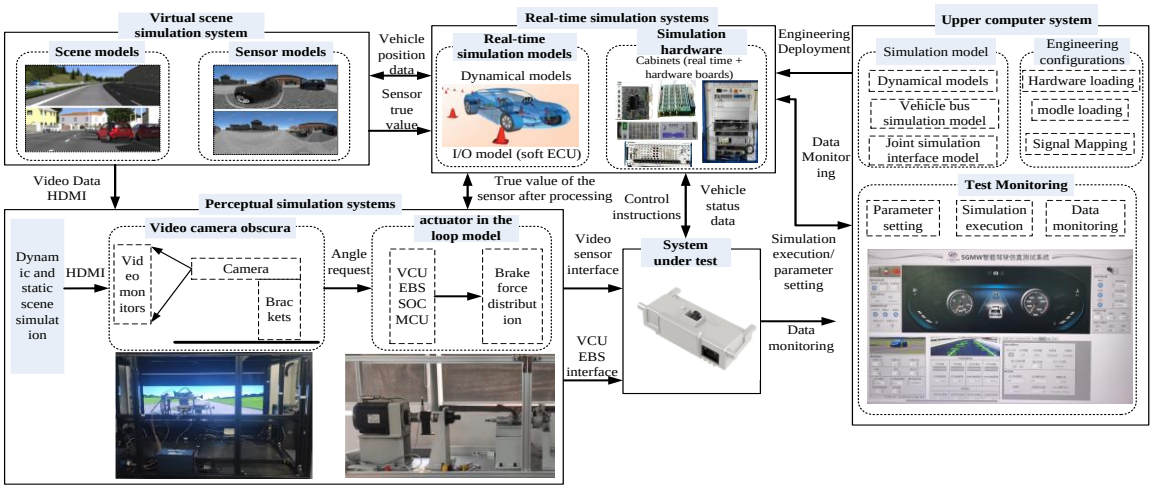

Figure 3. Hardware simulation environment

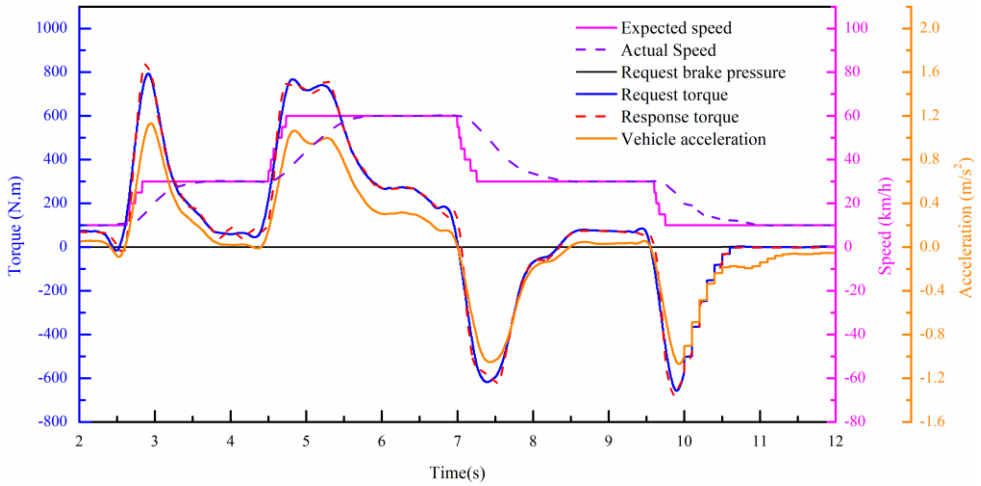

Figure 4. Comparison of simulation results for cruise control conditions

The stop-go conditions test the safety and following ability of the system. Figure 5 compares the acceleration and distance when following vehicle with the design values. The requested acceleration and design acceleration trends are well aligned, with peak deviations within 3% and good accuracy. The smooth decrease and increase of acceleration prove that the logic of torque and brake pressure switching during acceleration and deceleration is in line with the design. The actual distance between vehicles can stably follow the changes in the safe distance between vehicles, and the deviation between the actual distance and the design value during the following process is within 0.6m. The average distance for stopping is 3.2m, which meets the system's requirement for following and stopping distance (3 ± 0.5m).

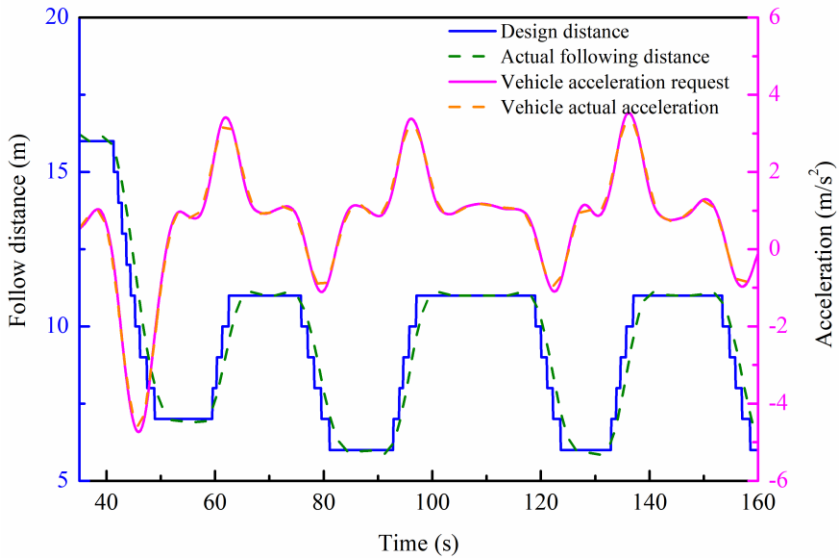

Figure 5. Comparison between following distance and design value simulation

Figure 6 shows a comparison of the simulation results of torque and pressure changes during the stop and go process. From the speed change curve, the self-driving vehicle follows the preceding vehicle to achieve start, acceleration, deceleration, and braking. Point A is when the vehicle decelerates from 90kph, starting with negative torque deceleration. After reaching the maximum negative torque limit of the system, pressure braking is applied, and the acceleration smoothly transitions throughout the process as shown in Figure 5. Point B is during the process of starting and stopping, first requesting negative torque for braking. When the speed is below 12kph, the system directly requests pressure braking and synchronously requests torque release to 0. The entire process involves smooth torque switching, rapid pressure rise, smooth acceleration transition between torque and pressure, and no jerking of the entire vehicle. It can be seen that the ACC control strategy controls the vehicle to safely and smoothly follow the target vehicle ahead under stop and go conditions, and always maintains a safe distance from the target vehicle ahead, with good followability and safety.

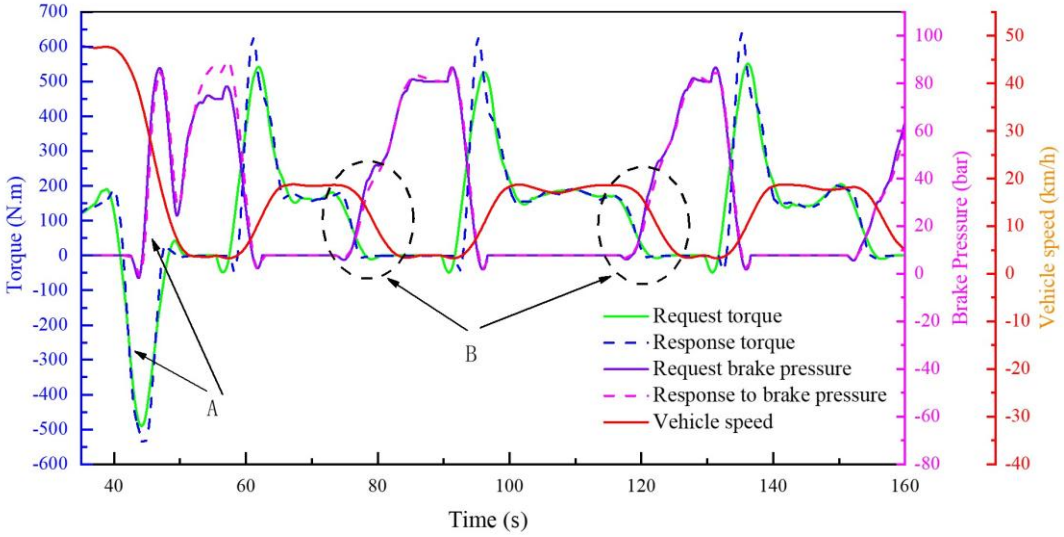

Figure 6. Comparison of simulation results of torque and pressure changes during the stop and go process

The simulation results show that in various scenario tests, the intelligent driving braking energy system of model predictive control can accurately achieve acceleration and uniform speed control by controlling the motor, and can also achieve deceleration control through motor torque and pressure braking. The control follow-up effect is good, which can effectively verify that the system has complete control stability and can meet the functional testing requirements of ACC system.

REAL VEHICLE TESTING VERIFICATION

Install the ACC system on a certain vehicle model to verify the effectiveness of the system design and actual energy-saving effects. Verify the rationality of the braking energy recovery control strategy through actual vehicle scenarios such as cruise control, stop-go, cruise following, and front car plugging. Verify the energy-saving effect of adding braking energy recovery strategy control in ACC mode through CLTC scenarios.

Verification of Braking Energy Recovery Control Strategy

Figure 7 shows the actual vehicle test results of a pure negative torsional deceleration scenario. The driver operates the control button to decelerate from 80km/h to 60km/h, 40km/h, and 20km/h. From the two sets of curves, can see that from the moment the requested torque is sent to the time when the actual torque responds, which is ≤ 50ms, the silence time delay is relatively small. The time from the moment of requesting torque transmission to the actual torque reaching 95% of the requested torque is ≤ 100ms, and the request response delay is small. The difference between the maximum actual torque and the requested torque is less than 5N. m, and the overshoot is less than 5%. Steady state error: The difference between the actual torque and the requested torque after stabilization is less than 5Nm, the system has a good steady state and there is no oscillation phenomenon under steady state. During cruising and coasting, the system uses negative torque from the motor for deceleration, resulting in a smooth and linear deceleration of the entire vehicle, with comfortable and precise control.

Figure 8 shows the results of a real vehicle test of negative torque & brake pressure hybrid deceleration. When the system decelerates slightly following the preceding vehicle, such as at point A, the negative torque requested for braking decelerates, and the deceleration & negative torque slope is small, in a stable deceleration process. As the preceding vehicle rapidly decelerates, the system requests an increase in deceleration and slope. The system cannot meet the requirements by relying on negative torque deceleration. At this time, the negative torque quickly pulls down to the maximum value, and at the same time, the combined request pressure enters the hybrid braking mode. From the acceleration response curve of the entire vehicle, it can be seen that the negative torque & pressure hybrid deceleration switch is timely. When the two are combined for deceleration, the driving torque tracking silence time of the VCU response is basically less than 100ms, the overshoot is less than 10N. m, and the tracking error is about 150ms. EBS has excellent response pressure tracking, with a maximum quiet time of 98ms, overshoot of less than 5%, tracking error of around 135ms, smooth acceleration curve of the entire vehicle, smooth speed drop, and no jerking during deceleration. The control comfort and accuracy are high.

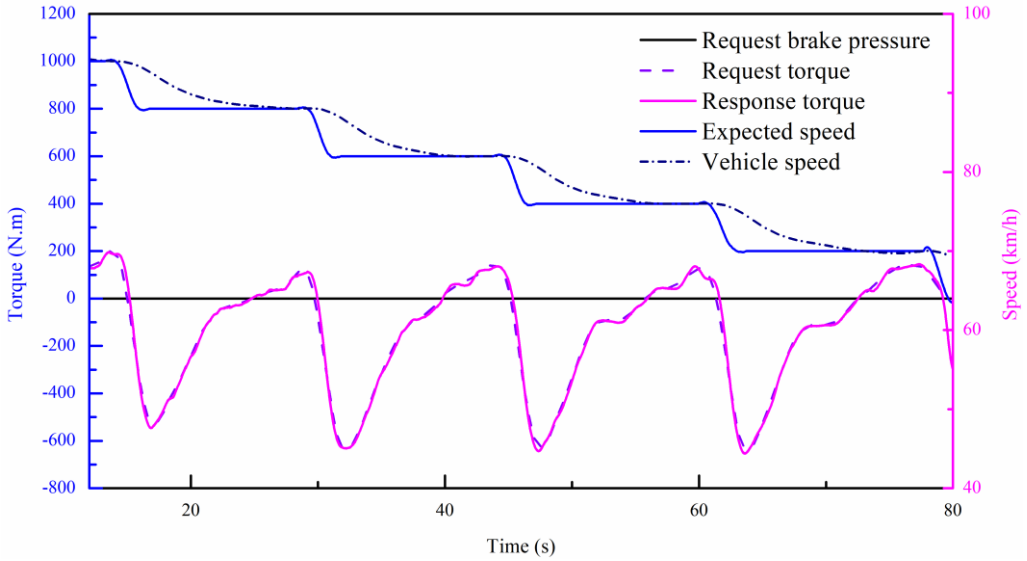

Figure 7. Real vehicle test results of pure negative torsional deceleration scenario

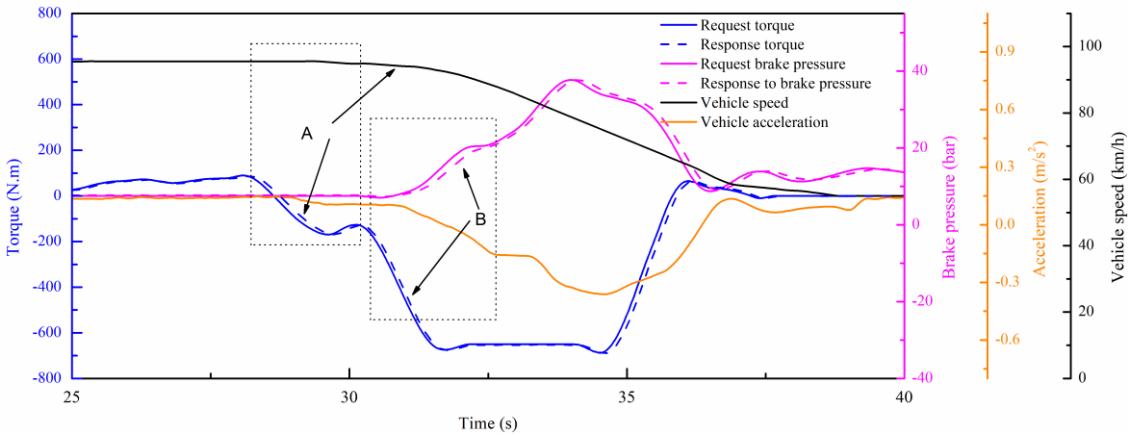

Figure 8. Real vehicle test results of negative torque & brake pressure hybrid deceleration

When the current vehicle is subjected to extreme congestion or sudden braking, the situation is critical. If negative torque braking is applied to the motor, the deceleration will slow down and there is a risk of collision. To avoid delayed deceleration and collision risk, the system directly requests pressure braking. Figure 9 shows the test results of pure pressure braking on a real vehicle. From the box in the figure, it can be seen that when the system performs rapid deceleration, it will quickly request torque release, maintain torque at 0, and the torque tracking error is less than 100ms. At the same time, the system quickly requests pressure braking, and the silence time is basically 100ms, with almost no overshoot generated. The entire process involves untwisting, natural switching of pressure braking connection, smooth and rapid deceleration, and no jerking during the deceleration process, which can meet the safety braking requirements in emergency situations.

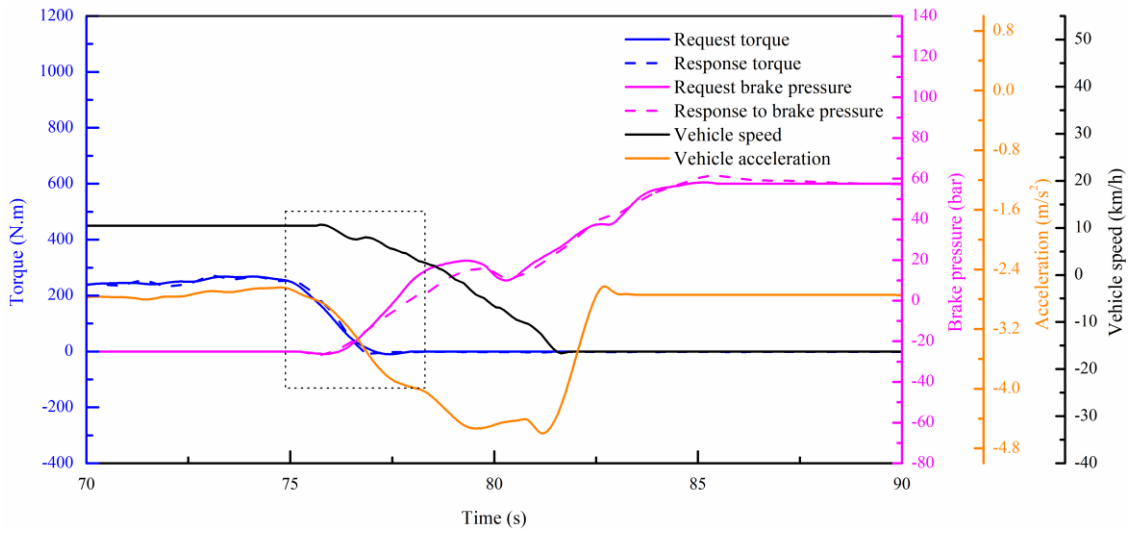

Figure 9. Real vehicle test results of pure pressure braking

Energy Saving Improvement Verification

Endurance mileage verification

According to the CLTC operating conditions, conduct road tests of approximately over 2000km in congested urban areas (40km/h-60km/h), suburban expressways (60km/h-80km/h), and highways (80km/h-120km/h). The initialization SOC power before each test is 100%, and the SOC power at the end of the test is 25%. Figure 10 shows the actual road test route of a certain vehicle model (theoretical range of 300) under reference CLTC working conditions, and Table 1 shows the actual vehicle test results under various scenarios.

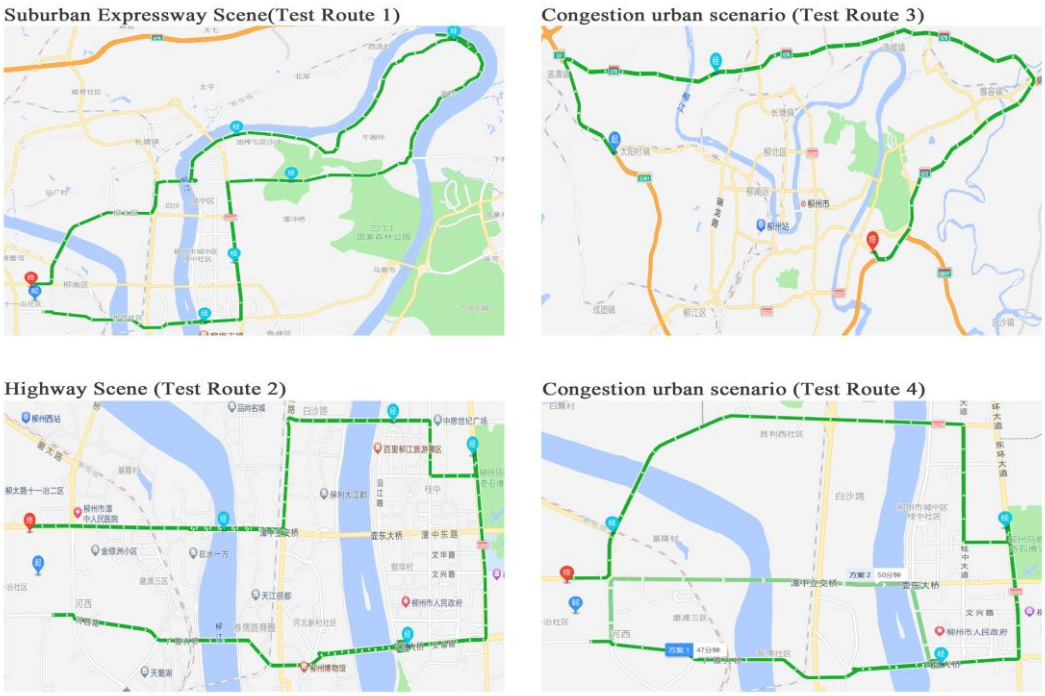

Figure 10. Actual road test route under CLTC conditions

Table 1. Real vehicle test results in various scenarios

Driving mode	Driving scene	Test mileage (km)	kwh/100 km	Maximum theoretical range (km)	Difference from theoretical range (km)
Before optimization (ACC)	Congested urban area	233	9.63	311.5	+11.5
	Suburban expressway	168	13.38	224.2	-75.8
	Highway	185	12.15	246.9	-53.1
Optimized (ACC)	Congested urban area	325.7	9.21	325.7	+25.7
	Suburban expressway	324.6	9.24	324.6	+24.6
	Highway	261.7	11.46	261.7	-38.3
Manual Driving	Congested urban area	230	9.78	306.7	+6.7
	Suburban expressway	198	11.34	264.5	-35.5
	Highway	196	11.49	261.1	-38.4

According to the weighted average of different test results, the overall range in ACC mode after optimization has increased by 16.9% compared to before optimization. Compared to manual driving mode, the overall range has increased by 9.7%. The energy consumption per 100 kilo meters has been reduced by 1.75 kwh, a decrease of 14.9%, and the energy-saving effect is significant. Figure 11 shows the endurance and energy consumption test results before and after optimizing the energy recovery mode.

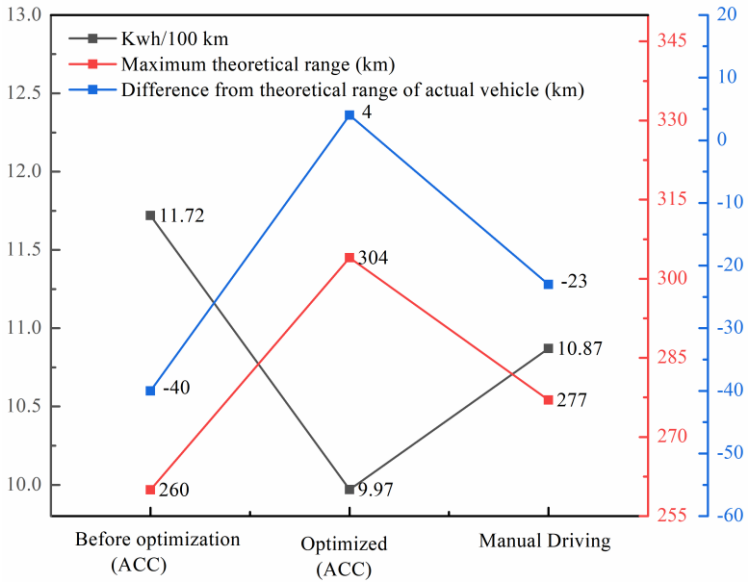

Figure 11. Increase the endurance and energy consumption test results before and after energy recovery

Optimization of braking performance

Based on the CLTC operating conditions and the frequent use of ACC braking in daily life, three different braking conditions were designed at different speeds: following the stationary target, dynamic following, and following deceleration. The brake verification scenarios and test results are shown in Table 2. EgoV is the speed of the ego vehicle, gvtF is the target vehicle speed, and the average weighted braking pressure and braking deceleration under similar operating conditions are taken.

Table 2 Braking verification scenarios and test results

Test scenario	Test conditions	Maximum deceleration before optimization (m/s^2)	Optimized maximum deceleration (m/s^2)	Maximum brake pressure before optimization(bar)	Optimized maximum brake pressure(bar)
Follow the stationary target	gvtV:0km/h egoV:30km/h	-1.125	-1.562	11.5	11.5
	gvtV:0km/h egoV:40km/h	-1.359	-1.359	10	10
	gvtV:0km/h egoV:50km/h	-1.937	-1.437	19	8.5
Dynamic Follow Stop	gvtV:60km/h-0km/h egoV:70km/h	-3.031	-3.125	29.5	26
	gvtV:40km/h-0km/h egoV:70km/h	-2.156	-2.039	19	13
	gvtV:30km/h-0km/h egoV:70km/h	-2.953	-2.578	27.5	19.5
Deceleratd following the car	gvtV:60km/h—50km/h egoV:70km/h	-0.906	-0.937	9	4.5
	gvtV:60km/h—40km/h egoV:70km/h	-1.171	-1.203	10	7.5
	gvtV:60km/h—30km/h egoV:70km/h	-1.281	-1.312	10	7

Figure 12 shows the comparison of the average deceleration test results before and after increasing energy recovery. It can be seen that the deceleration sensation is further weakened: during dynamic and static braking processes, the overall deceleration of the optimized system is about 0.2m/s^2 lower than the average deceleration before optimization. The reduction in average deceleration further reduces the overall energy consumption of the vehicle.

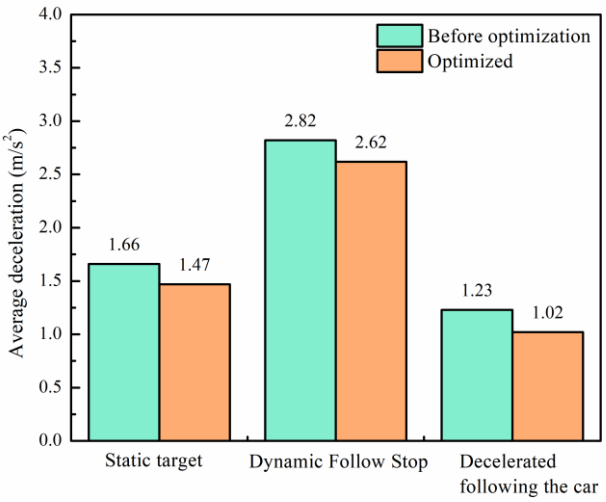

Figure 12. Real vehicle test results of average deceleration before and after increasing energy recovery

Figure 13 shows the actual vehicle test results of the average brake pressure before and after increasing energy recovery. It can be seen that the maximum brake pressure issued by the actual vehicle is reduced by about 4 bar on average, further avoiding brake energy loss.

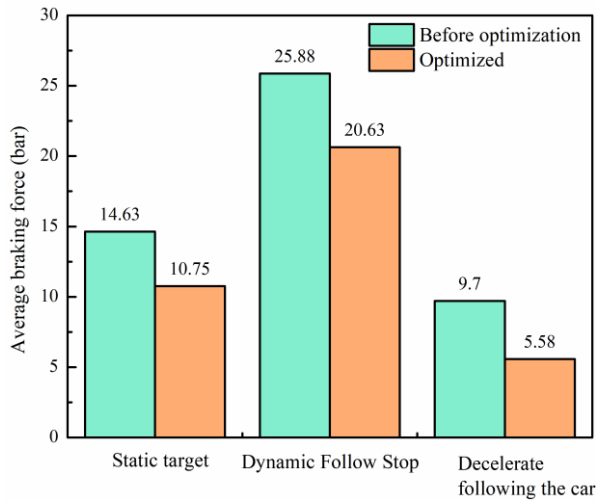

Figure 13. Real vehicle test results of average brake pressure before and after increasing energy recovery

According to the upper and lower limits of ACC acceleration and acceleration change rate specified in ISO 15622, ISO 22179, and i-VISTA, combined with subjective industry evaluations and OEM indicators, the reference acceleration absolute value is less than or equal to 1.1 m/s^2, and the acceleration change rate absolute value is less than or equal to 0 Experience of Comfort Evaluation with Good ACC Function and Physical Perception at 0.6m/s^3[19-21]. Figure 14 shows the statistical results of longitudinal acceleration before increasing energy recovery, and Figure 15 shows the statistical results of longitudinal acceleration change rate before increasing energy recovery. It can be seen that before increasing energy recovery, the absolute value of comfort perceived acceleration accounted for 86.7%, and the absolute value of acceleration change rate accounted for 88.1%. Figure 16 shows the statistical results of longitudinal acceleration after increasing energy recovery, and Figure 17 shows the statistical results of longitudinal acceleration change rate after increasing energy recovery. It can be seen that

after increasing energy recovery, the absolute value of comfort perceived acceleration accounted for 92.3%, an increase of 6.46%, and the absolute value of acceleration change rate accounted for 93.3%, an increase of 5.90%.

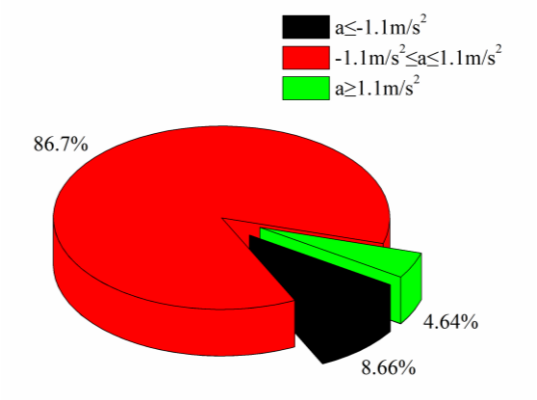

Figure 14 Increase longitudinal acceleration statistics before energy recovery

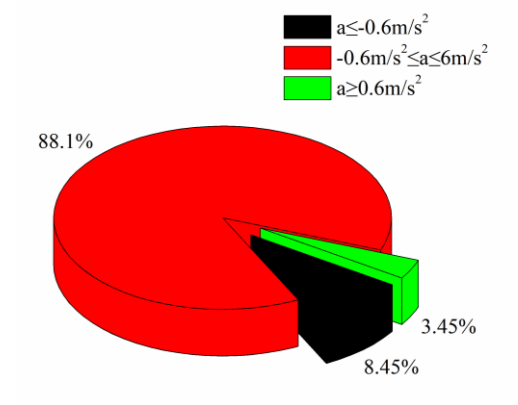

Figure 15 Increase the statistics of longitudinal acceleration change rate before energy recovery

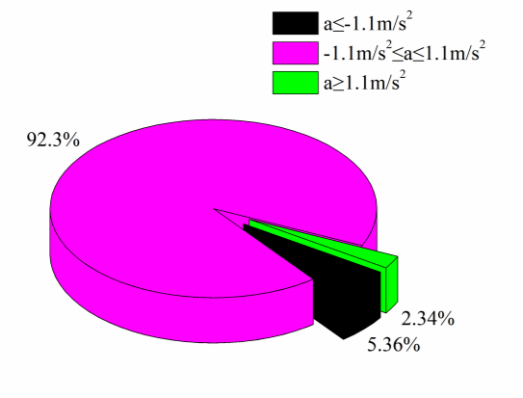

Figure 16 Increase longitudinal acceleration statistics after energy recovery

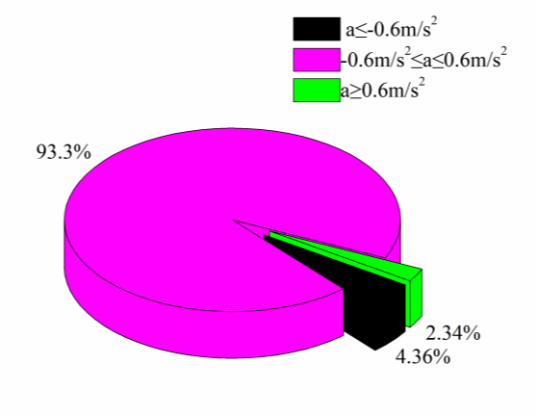

Figure 17 Statistical analysis of longitudinal acceleration change rate after increasing energy recovery

CONCLUSION

Improved control strategies and methods for intelligent driving and actuators, designed an intelligent driving braking energy system based on model predictive control, and verified its feasibility through a hardware in the loop simulation test platform built using Carsim/Veristand/MATLAB. At the same time, based on a certain vehicle model, CLTC working conditions and conventional cruise driving conditions were compared and tested in real vehicles, verifying that the system has safety and comfort, meets the requirements of mass production and installation, and can be extended to subsequent vehicle models.

1)Real vehicles demonstrate that in intelligent driving mode, when braking, the maximum utilization of VCU reverse drag braking is achieved by calibrating parameters and changing algorithm modes, reducing energy loss in mechanical braking and improving energy recovery efficiency.19

2)Intelligent driving has added an energy recovery mode, and after optimization, the overall range of intelligent driving has been increased by 17.5%. Reduce energy consumption by 1.75 kwh per 100 kilo meters.

3)Braking performance verification: The deceleration process is more linear: under small deceleration conditions, there is no need to apply hydraulic braking, and relying solely on motor reverse drag braking provides a more comfortable braking effect. Comfort level increased by 6.46%. The sense of deceleration is further reduced: during dynamic and static braking processes, the overall deceleration of the optimized system is 0.2m/s2 lower than the average deceleration before optimization. Optimization of braking force distribution: The average maximum braking pressure issued by the actual vehicle is reduced by an average of 4 bar, further avoiding braking energy loss.

ACKNOWLEDGMENTS

This work was supported by a project grant from four major science and technology projects in Guangxi:Guangxi Science and Technology Major Project (Guike AA23062030, Guike AA24206054, Guike AA24206056, Guike AA22068108).

REFERENCE

[1] Feng Li, Zhu Yunyao, Wu Shengnan, et al. Research on the Automated Supervision System for L2 Part of Intelligent Connected Vehicles. Automotive Digest, 1-5[2024-06-26].
[2] Li Tianjiao. Research on Multi Objective Optimization Adaptive Cruise Control Strategy for Pure Electric Vehicles. Jilin University, 2018.
[3] Chu Liang, Li Tianjiao, Sun Chengwei. Research on Adaptive Cruise Longitudinal Control Method for Pure Electric Vehicles. Automotive Engineering, 2018, 40(03): 277-282+296.
[4] Lu Y, Yang D, Yang J, et al. A comprehensive comparison of three desired acceleration calculation methods for mass production of adaptive cruise system. 2021 WRC Symposium on Advanced Robotics and Automation (WRC SARA). IEEE, 2021: 231-237.

[5] Li S, Li K, Rajamani R, et al. Model predictive multi-objective vehicular adaptive cruise control. IEEE Transactions on Control Systems Technology, 2010, 19(3): 556-566.
[6] Ren Jianxin. Research on Adaptive Cruise Control of Pure Electric Vehicles Based on Multi Objective Optimization. Beijing Jiaotong University, 2020. DOI:10.26944/d.cnki.gbfju.2020.002678.
[7] Li Yinong, Ji Jie, Zheng Ling, et al. Modeling and simulation of intelligent vehicle adaptive cruise control system. China Mechanical Engineering, 2010, 21(11): 1374-1381.
[8] Fancher P, Bareket Z, Ervin R. Human-Centered Design of an Acc-With-Braking and Forward-Crash-Warning System.Vehicle System Dynamics, 2001, 36(2-3): 203-23.
[9] Shakouri P, Ordys A, Laila D S, et al. Adaptive cruise control system: Comparing gain scheduling PI and LQ controllers. Proc. 18th IFAC World Congress, Milano, Italy, 2011, 2(1):1
[10] Moser D, Schmied R, Waschl H, et al. Flexible Spacing Adaptive Cruise Control Using Stochastic Model Predictive Control. IEEE Transactions on Control Systems Technology, 2017, PP(99): 1-14.
[11] Zhu M, Chen H, Xiong G. A model predictive speed tracking control approach forautonomous ground vehicles. Mechanical Systems & Signal Processing, 2016, 87: 25-27.
[12] Xie L, Luo Y, Zhang D, et al. Intelligent energy-saving control strategy for electric vehicle based on preceding vehicle movement. Mechanical Systems and Signal Processing, 2019, 130: 484-501.
[13] Zhang S, Luo Y, Li K, et al. Real-Time Energy-Efficient Control for Fully Electric Vehicles Based on Explicit Model Predictive Control Method. IEEE Transactions on Vehicular Technology, 2018, 13(99):1-1.
[14] Wentao H E, Defeng H E, Jinglong C, et al. Design of Verification Platform for Adaptive Cruise Control Algorithm of Connected Vehicles. Computer engineering and applications, 2019(7): 31-38.
[15] Sun Pengfei. Research on Start Stop Control of Adaptive Cruise Control (ACC) System for Automobiles. Jilin University, 2018.
[16] Fancher P, Bareket Z, Ervin R. Human-Centered Design of an Acc-With-Braking and Forward-Crash-Warning System. Vehicle System Dynamics, 2001, 36(2-3): 203-223.
[17] Yi K, Hong J, Kwon Y D. A vehicle control algorithm for stop-and-go cruise control. Proceedings of the Institution of Mechanical Engineers Part D Journal of AutomobileEngineering, 2001, 215(10): 1099-1115.
[18] Zhao D, Wang B, Liu D. A supervised actor-critic approach for adaptive cruise control. Soft Computing,2013,17(11):2089-2099.
[19] David J, Brom P, Stary F, et al. Application of artificial neural networks to streamline the process of adaptive cruise control. Sustainability, 2021, 13: 4572.
[20] Wu D, Zhu B, Tan D, et al. Multi-objective optimization strategy of adaptive cruise control considering regenerative energy. Proceedings of the Institution of Mechanical Engineers Part D Journal of Automobile Engineering, 2019(4): 11-15.
[21] Wentao H E, Defeng H E, Jinglong C, et al. Design of Verification Platform for Adaptive Cruise Control Algorithm of Connected Vehicles. Computer engineering and applications, 2019(7): 31-38.
[22] Ding Baocang. Theory and Methods of Predictive Control. Machinery Industry Press, 2008.